

# Live Cell Spinning Disk Microscopy

Ralph Gräf<sup>1</sup> (✉) · Jens Rietdorf<sup>2</sup> · Timo Zimmermann<sup>2</sup>

<sup>1</sup> A.-Butenandt-Institut/Zellbiologie, Ludwig-Maximilians-Universität München, Schillerstrasse 42, 80336 München, Germany  
rgraef@lrz.uni-muenchen.de

<sup>2</sup> Advanced Light Microscopy Facility, European Molecular Biology Laboratory, Meyerhofstrasse 1, 69117 Heidelberg, Germany

1	<b>Introduction</b>	58
2	<b>Principle of Operation</b>	60
3	<b>Comparison of Single Beam and Multi-beam Scanning Confocal Imaging</b>	61
3.1	Image Acquisition Rate	61
3.2	Efficiency, Photobleaching and Phototoxicity	62
3.3	Multichannel Imaging	63
3.4	Regional Bleaching	64
3.5	Optical Sectioning and Confocality	64
3.6	Conclusion	65
4	<b>Available Designs for Video-Rate Confocal Microscopy</b>	66
4.1	Multi-beam Designs	66
4.1.1	Laser-Based Spinning Disk Confocals	66
4.1.2	White Light Based Spinning Disk Confocals	66
4.1.3	Two-Photon Multi-Beam Scanning	66
4.2	Video-Rate Confocal Microscopes of Other Designs	67
5	<b>Single and Multi-Beam Confocal Imaging in the Analysis of Centrosome Dynamics in <i>Dictyostelium</i></b>	68
	<b>References</b>	72
	<b>Appendix</b>	73

**Abstract** In vivo microscopy of dynamic processes in cells and organisms requires very fast and sensitive acquisition methods. Confocal laser scanning microscopy is inherently speed-limited by the requirement of beam scanning movements. In contrast to single beam scanning systems, the parallelized approach of multi-beam scanning is much faster. Spinning disk confocal microscopes are therefore very suited for fast in vivo imaging. The principles of spinning disk microscopy will be explained in this chapter and a thorough comparison of the performance of single beam and multi-beam scanning systems is made and illustrated with an example of in vivo imaging in *Dictyostelium discoideum*.

**Keywords** Spinning disk microscopy · In-vivo imaging · Confocal microscopy · Real-time imaging

**List of Abbreviations**

AOTF	Acousto-optical tunable filter
AU	Airy disc unit
CCD	Charge Coupled Device
CLSM	Confocal laser scanning microscope
CSU	Confocal scanning unit
FRAP	Fluorescence Recovery after Photobleaching
GFP	Green Fluorescent Protein
MBCM	Multi-Beam Confocal Microscopy
NA	Numerical aperture
PMT	Photomultiplier Tube
SBCM	Single Beam Confocal Microscopy

**1****Introduction**

In biological imaging, confocal laser scanning microscopy (CLSM) has in the last decade significantly extended our ability to visualize highly complex samples as multidimensional datasets (space, time, colors). In parallel, the introduction of fluorescent protein variants as *in vivo* tags of structures of interest has opened up new ways to observe cellular processes inside the living cell or tissue (for review see Miyawaki et al., this issue).

In this chapter we will present and discuss a confocal microscopy variant that is very well suited to *in vivo* imaging.

The most common type of confocal microscope uses a single focused laser beam to sequentially point-scan a region (single beam confocal microscope, referred to as SBCM in the following text). The fluorescence created by the passage of this focused beam through the sample is sent through a narrow aperture in the intermediate image plane (the confocal pinhole) onto a detector and is thus reduced to the photons coming from the plane of focus of the objective, but not from regions above or below it (Fig. 1A). By this rejection of out-of-focus contributions an optical section is created containing only the information from the focal plane. This basic operational principle as it was already realized for Marvin Minsky's prototype in 1955 is used in most commercially available confocal microscopes today.

Long before confocal microscopes became a standard imaging tool in biology, however, another more parallelized approach to confocal imaging was developed using a technique significantly predating most electronic imaging inventions: In 1884 Paul Nipkow created a device that transmitted images electrically. It was the first television camera and made use of a rotating disk with a spiral pattern of holes that broke down two-dimensional information into a sequential series of signals that could be reconstituted into an image using a complementary disk with the same pattern.

In 1968, M. Petrán and his collaborators applied the Nipkow disk principle to develop a tandem scanning reflected light microscope in which the single

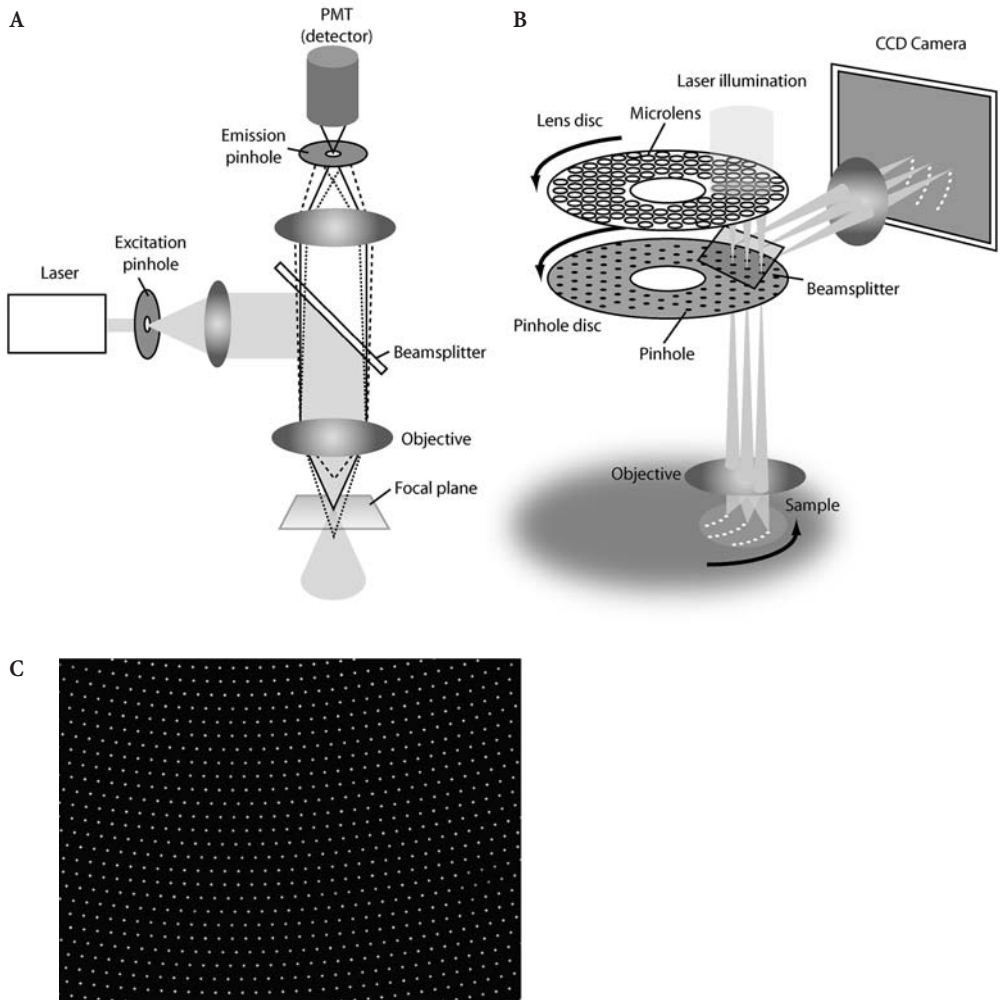


**Fig. 1A-C** Operating principles of single and multi-beam scanning confocal microscopes: **A** schematic drawing of a single beam scanning confocal microscope; **B** schematic drawing of a multi-beam scanning confocal microscope (Yokogawa CSU 10); **C** the constant pitch helical pinhole pattern of the Yokogawa spinning disk in the image field. During rotation of the disk, the pinholes evenly sweep the whole field of view

beam scanning confocal approach was parallelized to utilize multiple beams and corresponding pinholes [1]. Although this approach overcame the severe speed disadvantage of the single beam scanning method, it had significant problems of its own. For fluorescence imaging, the technology suffered from little excitation light reaching the sample due to the limited pinhole area (approximately 1%). Additional drawbacks were the requirement of high precision in the pinhole placement for designs with opposing excitation and emission

pinholes or problems with the scattered excitation light inside the detection system for setups using the same pinhole for excitation and emission [2].

When confocal microscopes became more widely available due to improvements in computer and imaging technology, the favored approach was single beam scanning. Recently, a significantly improved disk design by Yokogawa Inc. as well as progressive improvements in camera design have re-established the alternative multi-beam scanning technique (multi-beam confocal microscope, referred to as MBCM in the following text), especially for the requirements of in-vivo imaging. In combination with the Green Fluorescent Protein (GFP) technology applied in live-cell imaging, fast, multi-beam scanning microscopy is now a powerful tool for cell biology.

It is our aim in this chapter to explain the operational principle of multi-beam (tandem) scanning microscopy, to distinguish it from single beam scanning approaches, to compare their possibilities, to present commercially available designs and to demonstrate suitable applications.

## 2 Principle of Operation

The principle of operation of spinning disk microscopes will mainly be explained referring to a confocal scanning unit (CSU) designed by Yokogawa Corp [2]. It represents a very modern variant of the basic concept and in its design some of the initial limitations of the tandem scanning technology (little excitation light, uneven illumination, backscattering) were addressed and overcome. It is incorporated into several commercially available spinning disk setups (Perkin Elmer, VisiTeC).

A spinning disk confocal microscope consists of a rotating disk with multiple pinholes and a CCD camera (Fig. 1B). The pinholes on the disk (Fig. 1B) are arranged in a pattern that allows every location of an image to be covered when the disk is rotated.

In spinning disk microscopes an even field of illumination is created (e.g. by widening laser illumination into a circular field) that irradiates a section of the spinning disk (Fig. 1B). While most light does not pass the disk, the light going through the pinholes forms a set of minibeam corresponding to the pinhole pattern and sweeps the image field because of the disk rotation. Every mini-beam in itself is confocal, with the same aperture serving as the excitation as well as the emission pinhole for a single mini-beam (Fig. 1C, [2, 3]). Designs using opposing pinholes on the disk (Petran et al. 1968) are not realized in the current instruments.

In the Yokogawa design a constant pitch helical pinhole pattern is rotated in order to provide even and stripe-free illumination of the entire field of view. Of the 20,000 pinholes on the disk, approximately 1000 cover the field of view of the microscope at any time (Fig. 1C). Due to the pinhole arrangement, every single image position is covered with 1/12th rotation of the disk. As the disk

rotates with 1800 rpm (i.e. 30 rps) this amounts to  $30 \times 12 = 360$  full frames that are acquired per second [2].

To avoid crosstalk between the spots of individual minibeam, the pinholes are spaced significantly apart [3]. Accordingly, only a small area of the disk is covered by pinholes (1–4%) and most of the excitation light does not reach the sample because it is blocked by the disk. In the Yokogawa design this problem is overcome by a second disk in front of the pinhole disk (Fig. 1C). It contains microlenses arranged in the same pattern as the pinholes. These collect the excitation light and focus it into the pinholes thereby significantly increasing the excitation light throughput from approx. 1% to 40–60% [2].

A confocal image is formed almost instantaneously and can be directly viewed through the eyepiece of the scanhead.

In SBCMs, the emitted light is detected by photomultiplier tubes (PMTs) that read out intensities over time. Spatial information is not perceived. The image is reconstituted by plotting the intensity value of a certain time-point to the corresponding x-y-position of the scanning beam. MBCMs use a two-dimensional detector (a CCD camera) to record the intensity and spatial position of all minibeam simultaneously (Fig. 1B). The frame rate is defined by the camera exposure time and the frame readout speed of the camera. Maximally it can go up to 1/12 of the rotation frequency of the spinning disk (i.e. 360 fps in case of the CSU-10).

The characteristic differences between SBCMs and MBCMs consist in (1) serial against a parallelized scanning approach and (2) the mode of detection (PMTs vs CCD camera). All further differences between SBCMs and MBCMs result from these two initial factors.

### 3

## Comparison of Single Beam and Multi-beam Scanning Confocal Imaging

The following section will discuss how the differences in the images taken on both systems arise.

### 3.1

#### Image Acquisition Rate

In a SBCM the image acquisition rate is limited by the speed of the scan mirrors. The fastest scanning units currently available are operating at resonance frequency, thereby achieving 512-line-frame rates close to video rate or more than 100 Hz for reduced 32-line frame formats.

In a MBCM the image acquisition rate is limited by the speed of the camera readout. In the CSU-10 version of the Yokogawa scanhead the rotation frequency of the disc was limiting the acquisition rate to 360 Hz, which is no longer the case for the CSU-21 that can rotate with higher speeds.

As soon as light intensity becomes the limiting factor which is clearly the case for live specimen fluorescence imaging applications, images with similar

quality can be acquired much faster on a MBCM, due to its two- to fivefold overall higher efficiency (see below) and about 1000-fold higher integration time per pixel (pixel dwell time) allowing for higher light throughput per time unit without saturation of the fluorophore (see below).

To increase the image acquisition rate while keeping the light flux through the sample constant there are the principal possibilities to either sacrifice spatial resolving power or reduce the observed volume. Using the zoom function and changing the pinhole diameter the size of voxels and thereby resolving power of the system is easily and flexibly adjustable in the SBCM while in the MBCM the resolving power can only be changed stepwise by changing the objective, using an optovar or reading out the camera in binning mode (see also “Optical sectioning and confocality” below). In addition the SBCM can scan rather complexly shaped regions. Taken together, optimizing the observation volume is easier on a SBCM. This advantage however does not make the SBCM the superior tool for fast image acquisition except for applications where line regions are to be observed as for example in scanning a single line along an axon to measure the propagation of action potentials.

### 3.2

#### **Efficiency, Photobleaching and Phototoxicity**

According to theoretical estimates the overall light loss on optical components along the optical path of a filter based SBCM is expected to be similar to the loss inside the CSU10 based MBCMs (calculations according to [4], based on specifications in [5]), thus, differences in efficiency mainly rely on the different sensitivities of the detectors, which is in good agreement with our own findings and those of others [2].

The quantum efficiency of current CCD cameras (up to 75%) is significantly higher than that of PMTs (maximum 25% in most commercially available systems). Moreover, with the latest development of ‘on chip amplifying’ CCDs that achieve a strong amplification of the incoming signal while preserving a good spatial resolution, appropriate confocal acquisition of very fast biological processes inside living tissue has become feasible. While the higher efficiency in the detection of photons will reduce photobleaching and phototoxicity by making better use of the emitted photons, another advantage of MBCMs over SBCMs for live specimen imaging results from the higher efficiency in excitation of the fluorophores by the MBCM.

In single beam scanning, a high intensity laser beam passes over the sample and illuminates every region intensely, but only for a very short period of time (typically 2–3  $\mu\text{s}$ ). Only the light put into the sample and read out from the sample during this time is available to transport the information for the generation of the image. As a result, the excitation light has to be intense in order to excite enough fluorophores during this short time. In multi-beam scanning, the excitation light is split into many mini-beams of correspondingly lower intensity. However, several of these beams pass over the same region sequentially and the emis-

sion of all their passes is collected during the exposure time of the camera exposure. The illumination time per pixel is therefore significantly (1000-fold) longer.

We have analyzed the effects of these very different types of illumination by extending model calculations made by [6] for single beam scanning to a multiple beam situation (see Appendix at the end of the chapter).

We find that in the MBCMs significantly less excitation light is needed for the generation of an equivalent image due to two reasons: (1) the detection system is more efficient (see above); (2) the fluorophore saturation level is low. In SBCMs excitation light levels are close to the saturation of the fluorophore, a situation where the number of photons emitted by a fluorophore no longer increases proportionally with increasing excitation light intensity is easily reached, while in MBCMs the excitation light level is typically far from saturation of the fluorophore. The reduction of excitation light will at the same time also avoid potential photodamage by photochemical reactions independent of the fluorophore label (e.g. flavins) and in our opinion constitutes an additional important advantage for MBCM over SBCMs in the observation of living samples.

### 3.3

#### **Multichannel Imaging**

For many biological applications, the imaging of more than one fluorescence channel is required. This can be done on spinning disk systems by sequentially acquiring the different image channels onto the CCD and changing the excitation light and/or the emission filter between the channels. While switching between different excitation light lasers employing acousto-optical tunable filters (AOTFs) is fast (2 ms), changing emission filters involves filter wheels and is therefore ten times slower. Sequential multichannel acquisition involves a reduction in the image acquisition rate which can become a severe limitation for colocalisation studies of moving structures. Fast moving structures in the image might move between the acquisition of the channels and thus lead to mismatches between image channels.

Parallel acquisition is possible on MBCMs but requires modifications to the detection system. In such modified setups, the emitted fluorescence is split into longer and shorter wavelength components by a beamsplitter and either projected onto separate CCD cameras or onto different regions of the same CCD chip (DualView Beamsplitter). The recent introduction of sensitive color CCD cameras (like the Hamamatsu 3CCD camera) also has further potential for fast multichannel imaging (T. Nagai, personal communication) without significant alterations to the detection system.

Due to problems of significant crosstalk and cross-excitation between fluorophores (see review by Zimmermann in this issue), multichannel imaging is very often performed sequentially even on potentially parallel acquisition systems like SBCMs. By switching excitations line by line, SBCMs possess a sequential acquisition mode that avoids mismatches between channels, which is not available for MBCMs. For most applications, however, the subsecond

frame rates for multichannel imaging achievable on spinning disk confocals are adequate.

### 3.4 Regional Bleaching

Fluorescence Recovery after Photobleaching (FRAP) (for a review, see Houtsmuller in this issue) and photoactivation [7] or photoconversion of fluorescent proteins (see Miyawaki et al. in this issue) are powerful techniques to investigate protein dynamics inside living cells. These techniques require a bleaching or activation step, i.e. a short irradiation of a defined image sub-region with intense laser light and is easily performed on SBCMs. Although some spinning disk systems also use laser light for excitation, the laser cannot be used for spot or region bleaching in the existing setups. It is widened for the illumination of the whole field of view and cannot be specifically positioned within the image. Regional bleaching on spinning disk systems could however be performed with an additional positionable laser. This would require customization of the system, but it would be a formidable application considering the excellent fast time-lapse capacity of spinning disk systems.

### 3.5 Optical Sectioning and Confocality

The thickness of an optical section in a SBCM microscope can be varied by adjusting the diameter of the detection pinhole, while the pinhole diameter and therefore sectioning depth is fixed in MBCMs. The depth discrimination of the system is determined by the numerical aperture (NA) and magnification of the objective lens. For the CSU-10 from Yokogawa Inc. pinhole diameter and spacing are calculated to match a 1.4 NA 100 $\times$  lens for green excitation light and yield a 500 nm diameter projection of the pinhole in the object plane which is about 1 Airy Unit (AU) for an excitation wavelength of 550 nm and an optical section of about 0.8  $\mu\text{m}$  will be generated.

To achieve other section depths using the CSU-10, the investigator is limited by the available objective lenses. Using a 1.4 NA 60 $\times$  lens the projection of the invariant pinhole into the object plane will be larger than 1 AU resulting in a larger z-depth of 1.25  $\mu\text{m}$ . Using 1.3 NA 40 $\times$  the section is about 1.8  $\mu\text{m}$ . (For the Olympus DSU described below, discs with different optical properties are available to match the respective objective lenses and thereby higher flexibility is generated). Contributions of out-of-focus fluorescence into neighboring pinholes is to be expected in multi-beam systems depending on the fluorescence intensity and distribution inside the sample, thereby compromising their confocality [2]. Theoretical depth discrimination capability is therefore better in single beam setups. It should however be kept in mind that in order to achieve a high resolution excellent contrast is required which on a single beam confocal is usually difficult to achieve during live specimen imaging [8].



Under low signal to noise conditions the multi-beam confocal may achieve even better resolution due to its higher detection efficiency (see above).

### 3.6

#### Conclusion

Spinning disk microscopes are well suited for *in vivo* imaging and under certain conditions perform better than SBCMs for several reasons: (1) high frame rates can be achieved; (2) the use of CCD detectors provides high detection efficiencies; and (3) low intensity excitation light is used. Some of these advantages over SBCMs vanish if multichannel measurements are to be performed. Sequential acquisition compromises the advantage of fast acquisition and generates problems with respect to co-localisation studies while attempts to simultaneous acquisition using several cameras or beamsplitters are either tricky to align and expensive or severely compromise the light budget if emission beamsplitters or color cameras are employed. None of the commercially available variants of spinning disk microscopes are equipped for regional bleaching as required for photobleaching and photoactivation measurements. The overall resolution achieved of MBCMs is expected to be similar or better to that of SBCMs under low S/N condition as in live cell imaging due to higher detection efficiency. The main differences of the two system types are summarized in Table 1.

**Table 1** Overview of single and multi beam confocal microscope features for *in-vivo* imaging applications

Microscope type	Single beam confocal microscope	Multi beam confocal microscope
Acquisition speed	Limited frame rate +	High frame rate +++
Detection efficiency	Photomultiplier tube +	CCD camera ++
Bleaching rates for equivalent images	Higher, more emission photons required +	Lower, less emission photons required ++
Multichannel imaging	Simultaneous detection, sequential detection ++	Sequential detection +
Region specific bleaching	Possible ++	Not possible (w/o additional hardware) -
Optical sectioning, axial resolution	Adjustable pinhole diameter ++	Fixed pinhole diameter, possible crosstalk between neighboring pinholes +

## 4

### Available Designs for Video-Rate Confocal Microscopy

In this section a short overview over commercially available multi-beam scanning systems is given. In addition, other existing confocal designs that also provide high frame rates are briefly mentioned.

#### 4.1

##### Multi-beam Designs

##### 4.1.1

###### Laser-Based Spinning Disk Confocals

Since it is a self-contained solution, Yokogawa confocal scanning units (CSU) with the double disk design are employed in several commercial solutions (e.g. Yokogawa, Perkin Elmer, VisiTec, Solamere). In addition to the CSU-10, the more recent CSU-21 with higher disk rotation speeds and switchable filters is also available. The systems are operated with a variety of lasers and a CCD camera. For switching between fluorescence channels, solutions with filterwheels as well as with AOTFs exist. For simultaneous two-channel imaging, setups with two cameras are also available.

##### 4.1.2

###### White Light Based Spinning Disk Confocals

Two commercially available designs use Xenon or Mercury arc lamps for excitation instead of laser light. Because of the broad emission spectrum of the light source, the excitation light is controlled and easily varied by the use of excitation filters. This flexibility is not available with lasers as these are limited to specific excitation lines. They can be easily added onto an existing widefield system at relatively low cost and quick switches between widefield and confocal imaging are possible with them. They do provide images with improved z-resolution, but the optical sectioning capability is inferior to single beam scanning confocals due to restrictions in the light budget that are compensated by a decrease in confocality (see above).

The CARV module (ATTO Bioscience) contains a Nipkow disk with pinholes and can be added to a variety of widefield microscopes. The Olympus Disk Scanning Unit (DSU) can be fitted to Olympus microscopes and uses a rotating disk with a pattern of slits instead of pinholes. Its optical sectioning performance can be altered by the insertion of disks with different slit widths.

##### 4.1.3

###### Two-Photon Multi-Beam Scanning

A very different concept of multi-beam scanning is realized in Multifocal Multiphoton laser scanning Microscopy (TriM Scope, LaVision BioTec). In this

design a beam multiplexer is used to create an array of scanning foci (array can be single or rectangular/quadratic shape) that is used for parallel scanning at high rates. Functionally it is very different in that it uses multiphoton excitation to create its scanning foci and does not involve pinholes on the detection side. A similar multiphoton approach is provided by [9]. Time-multiplexed multifocal multiphoton microscopy overcomes the general problem of multifocal microscopy, crosstalk between single foci [10].

## 4.2

### Video-Rate Confocal Microscopes of Other Designs

In addition to multi beam scanning, other solutions for fast confocal imaging have been introduced over the years. With the increasing flexibility and speed of single beam scanning confocals many of them however have become obsolete and have gone out of manufacture. Slit scanning confocals [11] use a stripe of excitation light instead of a single point. As this stripe has to be moved across the sample in only one direction, scanning time per frame is significantly reduced so that images can be acquired at high frame rates with a CCD camera. The x-y resolution is however asymmetrical and the confocality is also compromised. Some existing commercial solutions (Meridian InSight, BioRad ViewScan DVC 250) are not manufactured anymore. Recently, Carl Zeiss AG has introduced the LSM 5 LIVE based on the slit scanning concept. Its distinguishing feature is a CCD line detector that allows very fast readout. Because of this, much higher frame rates at high scanning resolutions can be achieved than would be possible with a conventional CCD camera.

Fast scanning confocal microscopes increase the frame speed to video-rate by accelerated scanning of a single point. For this, either a resonant scanner or an acousto-optical deflector (AOD) is required [12]. The widely used Noran Odyssey XL employs an AOD for the fast scanning. Due to the AOD properties, the emission light cannot be completely descanned and has to pass through a slit instead of a pinhole aperture, thereby affecting confocality. The model is not produced anymore, but VisiTech International has recently introduced the VTeye based on the same concept. As a third way, Leica incorporated the resonant scanner approach into its existing range of confocal microscopes to offer a fast, fully confocal spectral setup (TCS SP2 AOBS RS). The limitation here is only in the zoom-in properties, as zooming can only be done centred due to the resonant scanner properties. As the imaging properties are like for any single beam scanning confocal, the comparison to spinning disk designs is as described above, but with higher frame rates gained at the cost of less detected photons.

## 5 Single and Multi-Beam Confocal Imaging in the Analysis of Centrosome Dynamics in *Dictyostelium*

The analysis of centrosome dynamics in *Dictyostelium discoideum* by four-dimensional imaging is a good example for an imaging task where three-dimensional movements of motile, small, fluorescent particles such as centrosomes have to be recorded over time.

The centrosome is a nucleus-associated organelle that serves as the main microtubule-organizing center in animal, plant and fungal cells. Its functions include mitotic spindle organization, cytokinesis, cell cycle progression, organelle positioning and the directionality of cell migration [13]. The centrosome duplicates once per cell cycle and the two centrosomal entities are separated during mitotic spindle formation where they are forming the spindle poles. The control of centrosome number, i.e. one per nucleus, seems to be essential for dividing cells to maintain their euploid state, since centrosome amplification leading to supernumerary centrosomes is a hallmark of tumor cells [14–16]. *Dictyostelium* amoebae are a good model system for centrosome research [17]. Thus, we have created a *Dictyostelium* mutant characterized by green fluorescent supernumerary centrosomes and a weak cytokinesis defect [18, 19]. This was achieved by overexpression of DdCP224, a member of the XMAP215-family of microtubule-associated proteins. The chromosomes in these mutants were visualized by co-expression of GFP-tagged histone2B. These mutants were used to investigate the dynamics of supernumerary and nucleus-associated centrosomes during mitosis [19]. The microscopic setup had to meet several requirements. The small size of *Dictyostelium* centrosomes (diameter of approximately 0.5  $\mu\text{m}$ ) requires the good spatial resolution of a confocal microscope. Their motility demands good temporal resolution and rapid acquisition of z-stacks over time, since the green-fluorescent centrosomes tend to move out of the confocal plane. Furthermore, *Dictyostelium* cells are very sensitive to phototoxic effects, especially during mitosis and if they are exposed to blue light required for GFP-excitation. Therefore, this was a suitable imaging problem to analyze differences in performance of spinning disk confocal microscopy (Perkin-Elmer-Wallac Ultraview) and single beam scanning confocal microscopy (Zeiss LSM510 META).

Since mitotic progression was inhibited by illumination with too high light intensities, long before any bleaching effect of GFP was detectable, the prevention of phototoxic effects turned out to be the most important task, independent of the imaging system used. Therefore, low laser powers had to be used which implied different consequences. In the case of spinning disk microscopy, relatively long exposure times of 500 ms and 2×2 binning had to be used resulting in a relatively low frame rate of approximately 1.3 frames/s and reduced pixel resolution. In the case of single beam laser scanning microscopy, low fluorescence signal intensities at a given laser setting require either high PMT voltages, which increases image noise, or a larger pinhole diameter, which de-

creases resolution. The frame rate depends on scanning options, such as the window size (in pixels), scan speed, bi- or unidirectional scanning, averaging of accumulated scans or the use of a line step (e.g. scanning of every second line with interpolation of the missing ones). To reach a rate of 1.3 frames/s a relatively small window size of 512×256 was chosen and the scan speed was set to the maximum. A line-step factor of 2 compensated the time needed to average two scans of each line, which was necessary to reduce noise.

It was not possible to compare the two confocal systems with the same laser power settings since both systems employ different lasers and filter sets. Therefore, settings were chosen which allowed viewing of the cells for at least 30 min without indications for phototoxic effects.

Both types of scan-heads were mounted on an inverted microscope and, therefore, glass-bottom petri dishes were used to view the cells. After the cells had settled on the glass surface (~5 min), the medium was replaced by phosphate buffer and the cells were flattened by agar overlay [20]. This reduced the high mobility of centrosomes in the z-direction and the number of z-levels required to follow the centrosome. The time delay between each stack was 10 s. Under these conditions, the *Dictyostelium* mutants were viewed at 21 °C for up to 30 min.

The image series shown in Fig. 2 represent maximum intensity projections of image stacks acquired with each of the two confocal systems. Both sequences show mitotic progression of a cell with GFP-labeled spindle poles and supernumerary centrosomes (arrowheads at time-point “0 s” in Fig. 2) as well as GFP-labeled chromosomes. Figure 2A shows a mononucleated cell with one supernumerary centrosome and Fig. 2B a bi-nucleated cell with two supernumerary centrosomes. Imaging started in early (Fig. 2A) and late (Fig. 2B) metaphase, respectively, with a bipolar mitotic spindle and chromosomes arranged in a metaphase plate. The supernumerary centrosomes are not involved in spindle dynamics but duplicate in anaphase (time-point “320 s” in Fig. 2A and “180 s” in Fig. 2B). Both sequences illustrate essentially the same process, but the image sequence obtained by spinning disk microscopy reveals more details regarding the discernibility of the chromosomes and the duplication event of the supernumerary centrosomes, where a tiny spindle is visible between the two daughter centrosomes (Fig. 2A, time-point “360 s”). By contrast, the images obtained by single beam laser scanning microscopy are noisier and less detailed (Fig. 3). The chromosomes, for instance, mostly appear as one mass instead of individual entities. This is due to the chosen compromise between speed, sensitivity and resolution. Improvement of any of the factors would have to be done at the cost of another. For example, taking out the line step to improve the y-resolution would have to be compensated by deactivating the line-averaging to maintain the same frame rate, thus leading to even more noise in the image. However, the scientific question, if and when supernumerary centrosomes duplicate, is solved equally well by both time-lapse sequences, although the spinning disk movie is of higher quality.

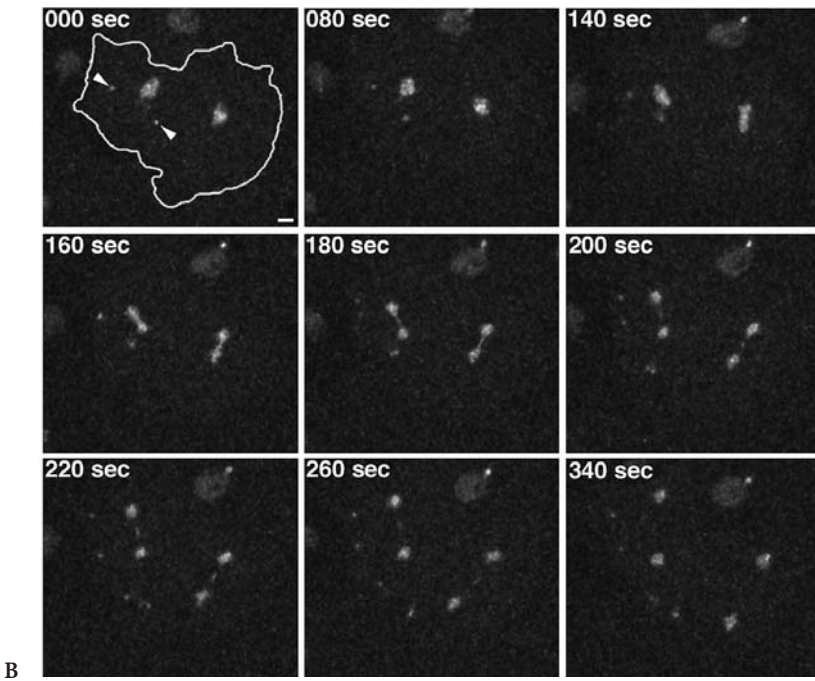
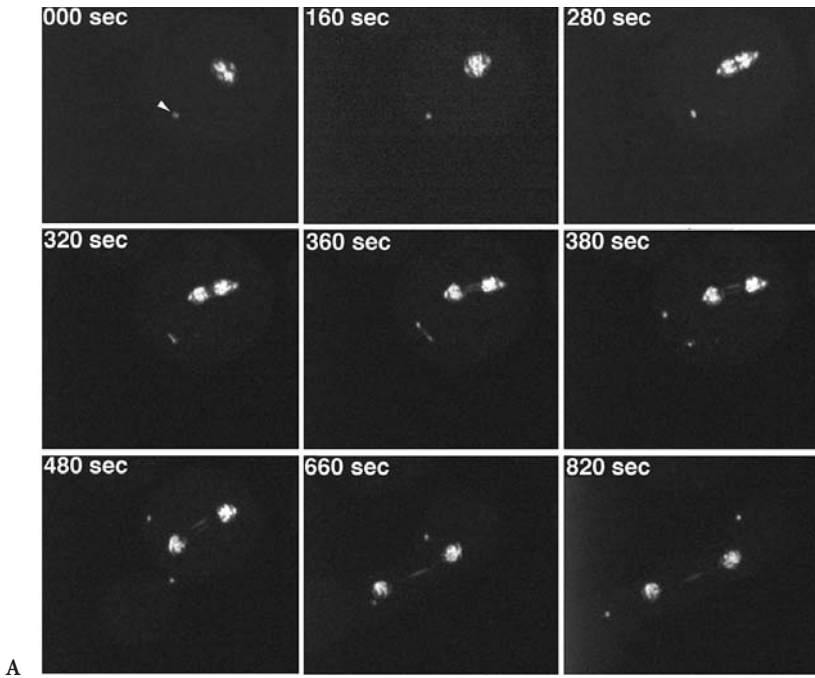


**Fig. 2A, B** Comparison of the duplication of supernumerary centrosomes as acquired on a spinning disk confocal microscope (Perkin-Elmer-Wallac Ultraview) and a single beam laser scanning confocal microscope (Zeiss LSM510 META): **A** spinning disk confocal (MBCM). Live observation of a mitotic DdCP224-GFP/GFP-histone2B cell with initially one supernumerary centrosome (*arrowhead in the first image*). Image acquisition started in late metaphase after duplication of the nucleus-associated centrosome whose daughter centrosomes are located at the spindle poles. The time is indicated in seconds. Each image represents a maximum intensity z-projection of five confocal slices. Settings: z-distance, 0.5  $\mu\text{m}$  each; exposure time, 500 ms; frame rate, 1.3 fr/s; binning, 2 $\times$ 2; **B** single beam confocal (SBCM). Live observation of a mitotic DdCP224-GFP/GFP-histone2B cell (cell edges are outlined in the first image) with initially two supernumerary centrosomes (*arrowheads in the first image*). Image acquisition started in late metaphase. The time is indicated in seconds. Each image represents a maximum intensity z-projection of five confocal slices. Settings: z-distance, 1  $\mu\text{m}$  each; 512 $\times$ 256 pixels; line-step, 2; averaging, twofold; pinhole size, 2.8 airy disk units; scan direction, unidirectional; scan speed, maximum; frame rate, 1.3 fr/s; *scale bars* 2  $\mu\text{m}$

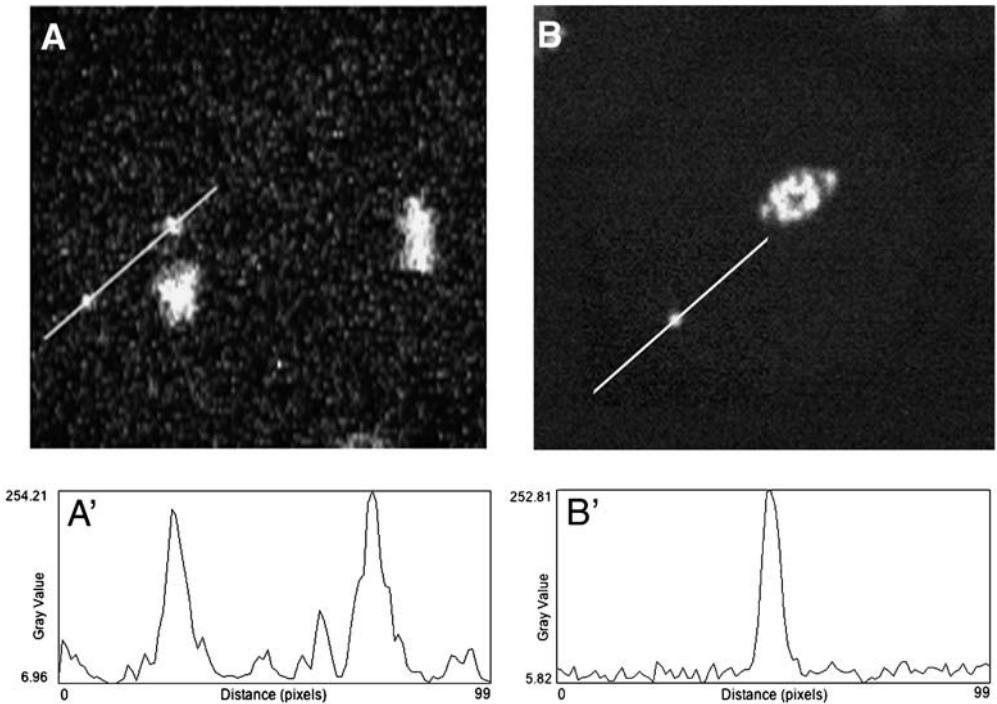


**Fig. 3A, B** Comparison of signal to noise ratio between laser scanning confocal microscopy and spinning disk confocal microscopy. Single slices derived from the image sequences of Fig. 2 are shown in A and B. The respective plots of fluorescence intensity (*displayed as gray levels of an 8-bit gray scale*) along a straight line through the center of supernumerary centrosomes (A', B') reveal superior signal to noise ratio of spinning disk microscopy vs single beam scanning microscopy

In cases of stronger signals, the frame rate (by shorter exposures) or the resolution (by reduction of binning) can be improved accordingly for spinning disk microscopes. At the single beam scanning microscope the frame rate used above is already close to the limit for such imaging tasks since the scan speed was set already close to the maximum. It can only be further improved by bidirectional scanning or omission of frame or line averaging. However, all these steps will reduce image quality. All improvements of the image quality, such as slower scanning, averaging of more scans or relinquishment of the line-step factor will significantly reduce the frame rate.

## References

1. Petran M, Hadravsky M, Egger MD, Galambos R (1968) *J Opt Soc Am* 58:661
2. Inoue S, Inoue T (2002) *Methods Cell Biol* 70:87
3. Kino GS (1995) In: Pawley JB (ed) *Handbook of biological confocal microscopy*. Plenum Press, New York, p 155
4. Stelzer EHK (1995) In: Pawley JB (ed) *Handbook of biological confocal microscopy*. Plenum Press, New York, p 139
5. Kawamura S, Negishi H, Ostuki S, Tomosada N (2002) *Yokogawa Tech Rep Engl Ed* 33:17
6. Tsien RY, Waggoner A (1995) In: Pawley JB (ed) *Handbook of biological confocal microscopy*. Plenum Press, New York, p 267
7. Patterson GH, Lippincott-Schwartz J (2002) *Science* 297:1873
8. Stelzer EHK (1998) *J Microsc* 189:15
9. Bewersdorf J, Pick R, Hell SW (1998) *Opt Lett* 23:655
10. Egner A, Andresen V, Hell SW (2002) *J Microsc* 206:24
11. Amos WB, White JG (1995) In: Pawley JB (ed) *Handbook of biological confocal microscopy*. Plenum Press, New York, p 403
12. Tsien RY, Bacskai BJ (1995) In: Pawley JB (ed) *Handbook of biological confocal microscopy*. Plenum Press, New York, p 459
13. Rieder CL, Faruki S, Khodjakov A (2001) *Trends Cell Biol* 11:413
14. Fisk HA, Mattison CP, Winey M (2002) *Curr Opin Cell Biol* 14:700
15. Nigg EA (2002) *Nat Rev Cancer* 2:815
16. Doxsey S (2002) *Mol Cell* 10:439
17. Gräf R, Brusis N, Dauderer C, Euteneuer U, Hestermann A, Schliwa M, Ueda M (2000) *Curr Topics Dev Biol* 49:161
18. Gräf R, Dauderer C, Schliwa M (2000) *J Cell Sci* 113:1747
19. Gräf R, Euteneuer U, Ho TH, Rehberg M (2003) *Mol Biol Cell* 14:4067
20. Fukui Y, Yumura S, Yumura TK (1987) In: Spudich JA (ed) *Methods in cell biology*, vol 28. Academic Press, Orlando, FL, p 347
21. Dittrich PS, Schwille P (2001) *Appl Phys B* 73:829



## Appendix

For comparing single and multi-beam scanning we follow a model calculation made by [6] for single beam scanning of fluorescein at 1 mW intensity at 488 nm and extend it for multi-beam scanning.

The following values are being used:

- Laser power at 488 nm: 1 mW
- Objective NA: 1.25
- Peak excitation intensity in a Gaussian spot  $I=1.25 \times 10^{24}$  photons/cm<sup>2</sup>s
- Fluorescein optical cross section  $cs=3.06 \times 10^{-16}$  cm<sup>2</sup>/molecule
- Fluorescein lifetime rate constant  $k_f=2.2 \times 10^8$  s<sup>-1</sup>
- Fluorescein quantum efficiency  $Q_e=0.9$
- Fluorescein bleaching efficiency  $Q_b=3 \times 10^{-5}$

The photon emission rate of a fluorophore is determined by the intensity dependent excitation rate, the lifetime of the fluorophore and its quantum efficiency. The excitation rate and the fluorophore lifetime allow the calculation of the saturation of the fluorophore. The photon emission rate as well as bleaching rate is directly proportional to it.

$$\text{Excitation rate constant } k_a = cs \times I \quad (1)$$

$$\text{Saturation } S = \frac{k_a}{k_a + k_f} \quad (2)$$

$$\text{Emission rate } k_{em} = Q_e k_f S \quad (3)$$

$$\text{Bleaching rate } k_{em} = Q_b k_f S \quad (4)$$

### Total Sample Irradiation Per Frame

How much light goes into a sample for a single exposure in the two setups? For this, an identical laser source and identical frame rates are assumed for both systems. In single beam scanning, the beam moves with finite speed over all regions of the sample. The total irradiation  $R$  of the sample is thus the product of the intensity of the laser beam  $I$  and the total acquisition time  $t$  for a frame.

$$R = I \times t \quad (5)$$

The comparison to a multi-beam system is actually quite simple: With an identical laser, the same intensity  $I$  is emitted for the same acquisition time  $t$ . The difference in photons actually hitting the sample is just determined by the transmission efficiency  $E$  of the spinning disk.

$$R = I \times t \times E \quad (6)$$

For identical frame rates and laser powers, the difference of total irradiation between a single beam confocal and a Yokogawa scan head would thus be a factor of approx. 2 (efficiency  $E$  0.4–0.6).

## Fluorescence emission

With this difference of total irradiation how much fluorescence is actually collected? This involves two aspects, the amount of emission photons and the efficiency of detection. In single beam scanning at 1 mW excitation intensity, fluorescein molecules in the region of peak intensity are 63% saturated, i.e. only 37% are not excited at any given time according to 1 and 2. The fluorescence emission rate  $k_{em}$  amounts to  $1.26 \times 10^8$  photons/s according to 3.

In multi-beam scanning with a Yokogawa disk, the intensity of a single mini-beam is significantly reduced and can be calculated as

$$I_{multi\_beam} = \frac{I}{n_{pinholes}} \times E \quad (7)$$

For  $n=1000$  pinholes and a transmission efficiency  $E=0.5$ , the intensity of a minibeam would amount to 1/2000th of the single beam intensity.

The saturation level of fluorescein in such a mini-beam is 0.09% according to 1, 2 and 7. The fluorescence emission rate is  $1.72 \times 10^5$  photons/s according to 3.

Whereas the difference in excitation intensity between single and multi-beam scanning is 1:2000, the difference in emission is only 1:731. This means significantly higher excitation efficiency at low intensities. This is an effect of the decreasing numbers of fluorophores available in the unexcited state at high saturation levels.

## Fluorescence Emission Per Frame

With the fluorescence emission rates  $k_{em}$  of single and multi-beam scanning setups known, how many photons are actually emitted by a fluorophore in a single frame?

For single beam scanning, the amount of emitted photons per fluorophore per frame  $N_{em}$  is

$$N_{em} = k_{em} \times t \quad (8)$$

where  $t$  is the pixel dwell time of the beam. Using the calculation example and a pixel dwell time of 2.5  $\mu$ sec this amounts to 300 photons emitted by a single fluorophore per frame.

For a spinning disk, the calculation can not be performed with pixel dwell times and the number of beam passes, since these parameters (radial velocity, number of passing pinholes) vary over the image field according to the radial position along the disk. The product of beam dwell times and beam passes is however a constant over the whole field (even illumination).

To derive a value equivalent to the single beam pixel dwell time for a spinning disk microscope, the total irradiation of the image field per frame has to be divided by the number of image pixels to get a representative illumination

value for each pixel under even illumination. The division of this value by the intensity of a mini-beam provides the total time of illumination centered on a pixel and thus an equivalent to the single beam pixel dwell time.

Accordingly, for multi-beam scanning the amount of emitted photons per fluorophore per frame  $N_{em}$  is

$$N_{em} = k_{em} \times \frac{R}{n \times I_{multi\_beam}} \quad (9)$$

where R is the total illumination of the sample per frame according to 6 and n is the number of image pixels.

Using this calculation, approximately 420 photons are emitted by a fluorophore under multi-beam conditions per frame.

This is an idealized calculation assuming identical areas of illumination for the single and multi-beam setups. In reality, only 63% of the circularly widened excitation beam goes into the rectangular (1.3:1.0) detection area of the CCD, so that less excitation light is actually used in the multi-beam system than for the calculation. Taking this into account, approximately equal amounts of fluorescence photons can be expected for single and multi-beam systems.

### Bleaching Rates

The photobleaching of fluorophores by illumination is still a poorly understood process [6]. Assuming linear bleaching kinetics even at the high intensities present in single beam scanning, as indicated by fluorescence correlation spectroscopy data [21], equal amounts of photons emitted per frame mean that the bleaching rate is more or less equal in multi-beam scanning and in single beam scanning microscopy.